

TOWARDS THE PERFECT MEISSNER STATE: A MAGNETO-OPTICAL STUDY ON COMPETING PINNING CENTERS IN NIOBIUM

J. Kösze[†], O. Kugeler, D. Abou-Ras, J. Knobloch, Helmholtz-Zentrum Berlin, Germany
R. Schäfer, IWF Dresden, Germany

Abstract

Over the past years trapped magnetic flux has emerged as a main limiting factor of high quality factors in SRF cavities. Several studies investigated how the ambient magnetic field can be minimized or how the flux expulsion during the phase transition can be improved. We now present a study that targets the pinning centers which allow for the flux to remain inside the superconductor in the first place. Using magneto-optical imaging we were able to not only measure the amount of trapped flux but in addition we managed to image its distribution with a resolution in the order of 10 μ m and correlate it with electron backscatter diffraction maps. As a result we found that the grain boundaries did not play a major role as pinning centers nor did the crystal orientation influence the amount of trapped flux significantly. However, niobium hydrides which formed during the cooldown to cryogenic temperatures were found to enhance trapping.

INTRODUCTION

SRF cavities are operated in the Meissner state of the superconducting (sc) material. In theory, all magnetic flux should be expelled during the phase transition into this state. However, pinning centers inside the material hinder the vortices from leaving. They get trapped and dissipate power once exposed to the RF field [1].

Therefore, the only pathway towards high quality factor SRF cavities leads through the elimination of all vortices inside the sc material. Since a cavity cannot be shielded completely from any magnetic field, e.g. because of thermocurrents [2-4], its expulsion during the sc phase transition must be maximized.

Recent studies investigated the influence of cooldown conditions on the efficiency of flux expulsion. The impact of the cooling rate and of the temperature gradient over the material during phase transition was studied [2, 5, 6]. In addition, a strong correlation was found for efficient expulsion and the grain size of the analyzed niobium [5, 7]. The study in Reference 7 investigated the change in the overall amount of trapped flux depending on the treatment history, especially high temperature heat treatment. It was found that a high average grain size was correlated with maximized flux expulsion. The results suggested that grain boundaries acted as the main pinning centers in niobium. The conclusion is reasonable since grain boundaries are known to act as pinning [8]. Following this argument, a higher average grain size would lead to fewer grain boundaries per area unit and hence to reduced pinning. However, there was no *direct* evidence that the grain boundaries are

the main pinning centers. The high temperature heat treatment influences not only the morphology but also several other material properties which might impact flux trapping.

In this work, we report on a study using magneto-optical (MO) imaging adding further information. The detailed study can be found in Reference [9]. The investigation targets the distribution of trapped magnetic flux in niobium after it transitioned into the sc state with an applied magnetic field. This specific application of MO imaging is comparatively new. Previously, the method was largely applied to image flux penetration close to the critical field which occurs at several 10 mT [10, 11]. We now explore the field regime below 10 mT and focus on the trapped flux after field cooling.

Using MO imaging different pinning centers in the niobium used for SRF cavities are directly imaged and compared with one another. Furthermore, it is compared how the distribution of trapped flux changes before and after the heat treatment. The obtained information can be used to systematically reduce the flux trapping in the future.

METHOD

MO Imaging Setup

MO imaging commonly utilizes the Kerr and Faraday effects [12], which occur in materials with magnetic circular birefringence and dichroism. Niobium exhibits neither of the two effects hence an indicator material has to be used in order to image the trapped magnetic flux. The indicator is placed on top of the sample as shown in Figure 1.

Polarized light is used to image the magnetic stray field originating from the sample as it extends into the indicator material. It passes the indicator twice due to the mirror layer and the polarization is changed by the Faraday effect. The MO indicator features a ferrite garnet film with in-plane magnetic anisotropy as a detection layer. As a result, the imaged magnetic field is the projection onto the sensitive axis of the garnet. Furthermore, the black and white contrast in the final image does not correspond to zero and maximum field but to the two possible orientations of the indicator as is also indicated in Figure 1. The MO images presented here were acquired in a setup at IWF Dresden, Germany [13]. An in-plane indicator was used with magnifications of 2.5 and 20. Therefore, the resolution can be estimated to be approximately 10 μ m.

[†] julia.koeszegi@helmholtz-berlin.de

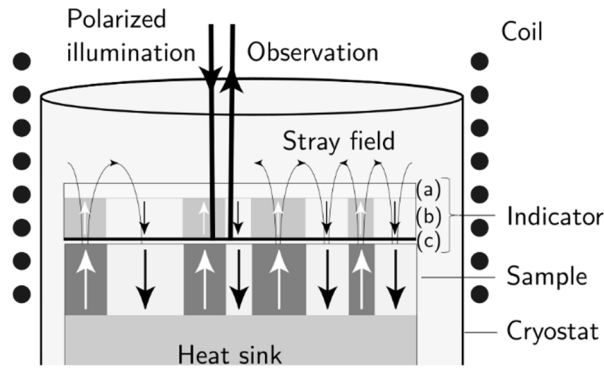


Figure 1: Magneto-optical setup with the Nb sample inside the cryostat. The coil applies the magnetic field during the sc phase transition. The indicator consists of (a) substrate, (b) the detection layer and (c) a mirror layer.

Measurement Sequence

The experiment started in the normal conducting state. A magnetic field was applied perpendicular to the sample surface. The sample was cooled below the critical temperature and it transitioned into the superconducting state. Thereafter the applied field was turned off. MO images were taken of each step. The complete sequence including the imaging (labeled (0), (A), (B), etc.) is shown in Figure 2.

Samples

Niobium with a RRR of 300 was provided by Heraeus. The material was cut from an ingot in discs with 10 mm diameter and 5 mm height. Sample 1 received no further treatment (ingot sample).

Sample 2 received a BCP where 95 μm material were removed from each side. The sample was heated at 1400°C. Finally, it was polished mechanically which is not a standard cavity treatment but was added to improve the sample smoothness for the MO imaging. The polishing was performed in five steps with silicone and diamond suspension of decreasing particle size. The last step included a H_2O_2 solution (100 ml + 10 ml).

RESULTS

Sample 1 (ingot)

Previous measurements showed that untreated, and especially unbaked, niobium trapped 100% of the applied field during the superconducting phase transition [5]. According to these measurements we expect complete trapping for sample 1. Figure 3 shows the result of the first test where the sample was cooled in a field of 10 mT. A magnification of 2.5 was chosen to balance the desired spatial resolution with the demand to get some overview over the sample.

The images show some noise in the grey values which will be discussed later. Despite the noise the figure shows clearly that the sample trapped close to 100% of the applied magnetic flux.

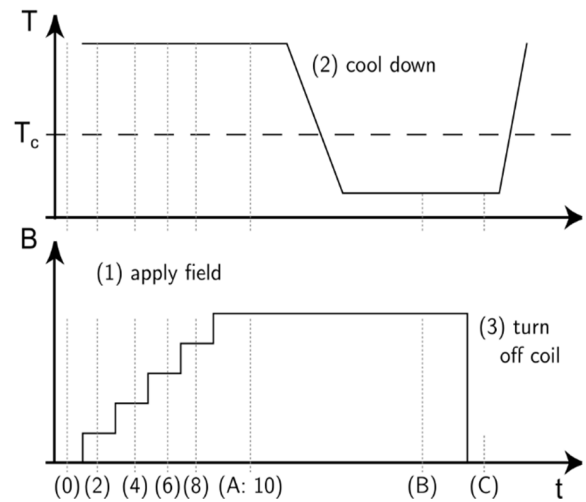


Figure 2: The magnetic field (2 to 10 mT) was applied before the sample was cooled below the critical temperature. MO images were taken previous to (A) and after (B) the phase transition. The magnetic field was turned off and the trapped flux inside the sample was evaluated (C).

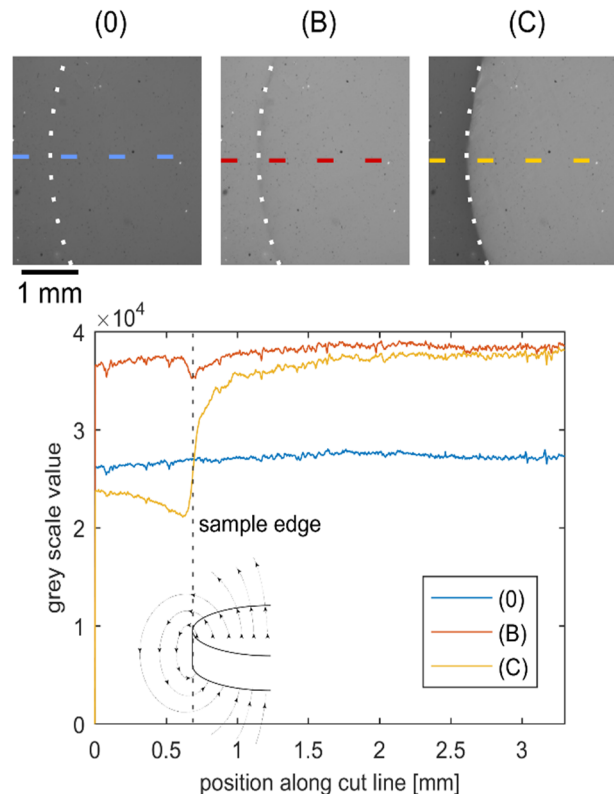


Figure 3: Trapped magnetic flux inside sample 1. 10 mT were applied during the cooldown. Upper row: The sample is shown before the field is applied (0) and in the superconducting state with coil on (B) and off (C). The white dots indicate the edge of the sample. The colored dashed lines show the cut lines.

Once the coil was switched off, the measured field over the center of the sample barely changed. The field outside the sample, however, changed its orientation because the magnetic field lines had to be closed. The field value approached zero with increasing distance from the sample

Content from this work may be used under the terms of the CC BY 3.0 licence (© 2017). Any distribution of this work must maintain attribution to the author(s), title of the work, publisher, and DOI.

edge. A small sketch indicating the orientation of the magnetic field originating from the sample is shown in the figure in addition. Due to the change in orientation, the grey scale values outside the sample in image (C) are smaller than the values for no applied magnetic field (image (0)).

The variation in the grey scale value in Figure 3 which appears to be noise mainly originates from the indicator. Since curve (0) was measured without an applied magnetic field, the variation in that data set cannot originate from trapped flux. We conclude that we observe artifacts introduced by the indicator limiting the resolution of the method. Many artifacts originate from the mirror on the bottom of the indicator which is scratched easily. At these positions, no magnetic signal from the sample can be obtained. The measured signal at all other locations is however not affected.

Sample 2 (1400°C heat treated)

For the second, heat treated sample, the field cooled measurement was again performed as described above. Since a mere comparison between images taken at time (B) and (C) provides only limited information, a calibration of the indicator was performed. Six images were taken prior to the cooldown in the normal conducting state. The applied field was increased from 0 mT to 10 mT in 2 mT steps as is indicated in Figure 2. The obtained data directly reflects the properties of the indicator material because the grey scale values correspond to the total rotation angle of the plane of polarization inside the detection layer at a given coil field. Since this material property cannot be modeled easily, a piecewise linear interpolation was chosen and performed independently for every pixels.

After the calibration images were taken, the sample was cooled below the transition temperature in ambient 10 mT and the applied field was switched off. The magnetic flux remaining trapped inside the sample was imaged and the grey scale image was converted into a magnetic field map by use of the previously taken calibration.

Figure 4 displays three images. First, the grey scale image of the sample obtained after the coil was switched off. Second, the magnetic field map calculated using the calibration curves. Third, the grey scale image with subtraction of a background image, which was taken before the phase transition.

As was already seen with sample 1, the image exhibits several artifacts which originate from the indicator. Most of them appear white in the magnetic field map due to the calibration. Furthermore, some artifacts are caused by the domains of the indicator material which cause the triangle-like shapes in the bottom left quadrant of the image [12]. The upper right corner displays the sample very close to its edge. Here, the magnetic field was around zero and started to point in the opposite direction outside the sample. Since the calibration was only taken above 0, these regions are also displayed white. Despite the artifacts several conclusions on the pinning can be drawn from the measurement which will be presented in the following.

First, we added the grain boundaries to the magnetic field map. The locations of the boundaries were extracted

from an optical microscope image of the surface taken prior to the MO measurement and are shown as red lines.

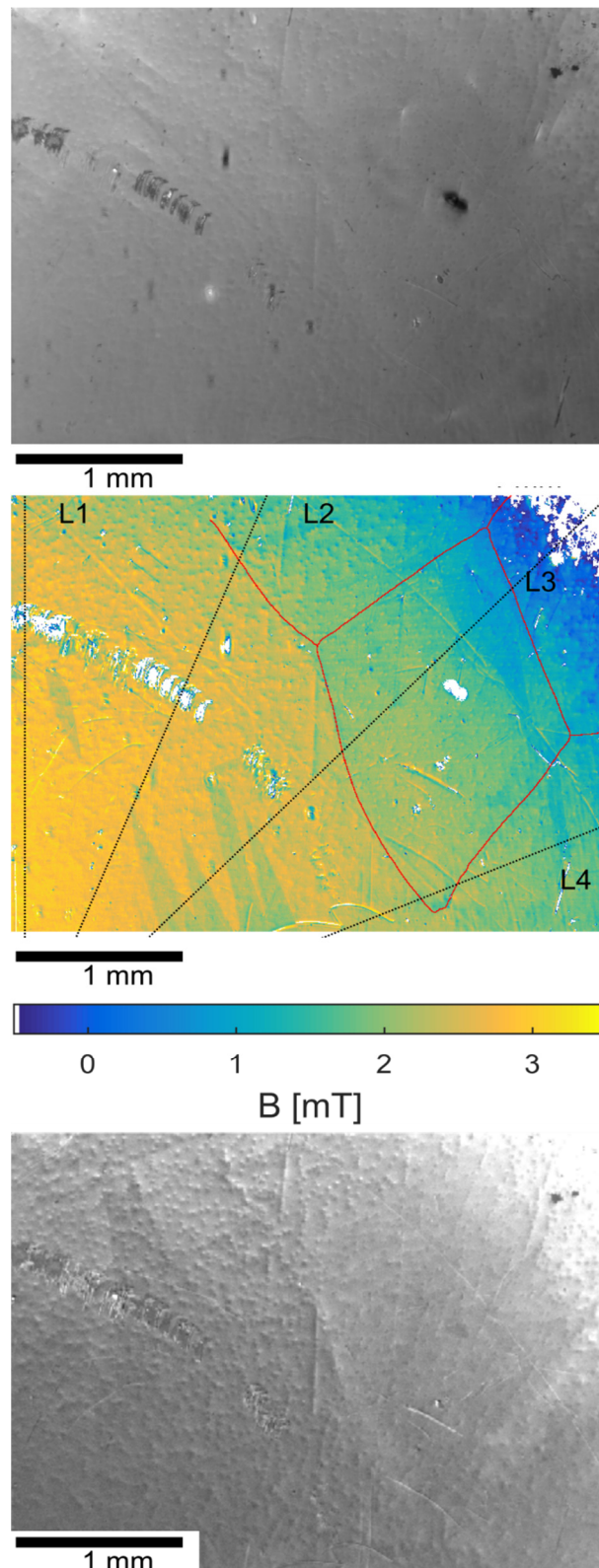


Figure 4: Trapped magnetic flux after cooling in 10 mT. top: Grey scale image, middle: Calculated magnetic field, bottom: top image with background subtraction.

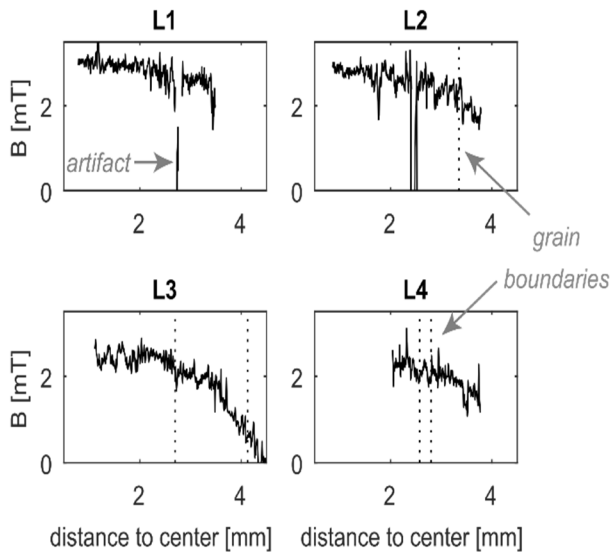


Figure 5: Magnetic field along the four cut lines. The dotted lines indicate the locations of grain boundaries.

In addition we drew black cut lines (L1 to L4) from the center of the sample towards the edge.

We see that the detected magnetic field decreased from the center of the sample towards the edge. Since the indicator measured only the stray field originating from the sample in the direction perpendicular to the surface the measured distribution can be caused either by an actual decrease of trapped flux towards the sample edge or by a geometry effect as was already seen in Figure 3. In any case, the upper limit of trapped magnetic flux is about one third of the applied magnetic field during cooldown. Hence, the sample exhibited drastically reduced trapping compared with sample 1, which is as expected.

As the next step, we evaluated possible changes of trapped magnetic flux between the grains and at the grain boundaries. The exported magnetic field values along lines L1 to L4 are shown in Figure 5. Once more we see that the measured field decreases towards the edge, however no significant difference in trapped flux is apparent: Neither at the grain boundaries nor from one grain to the other.

In this setup, we know that during the phase transition the superconducting phase grows from the center of the sample towards the edge. Thus, the measurement includes grain boundaries running at different angles relative to the progressing phase front. The values range from almost parallel (15°) to almost orthogonal (104°) and from none of the orientations a significant impact on the trapping was found.

These results indicate that the main pinning centers in the high purity, heat treated niobium might not be grain boundaries which contradicts our expectations based on the data in References 5 and 7.

In addition to the already discussed distribution of trapped flux, Figure 4 shows small structures which do not originate from artifacts or from the grain structure. More information can be gained by subtracting a background image, taken before the phase transition, from the data. The resulting image is shown in the bottom of Figure 4.

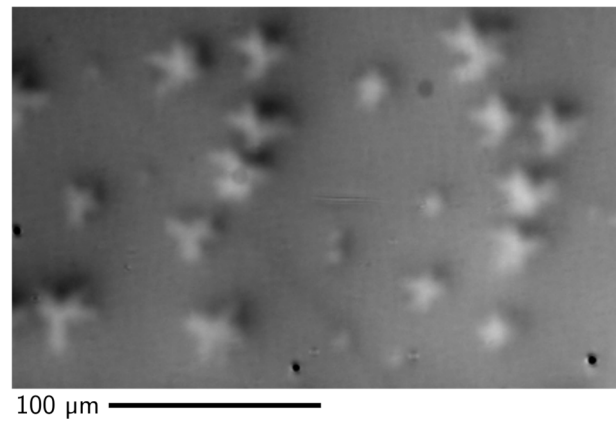


Figure 6: Pattern of trapped magnetic flux with magnification 20x.

In the image, dots become apparent. For further investigation, the structures were imaged with magnification 20 (Figure 6). The structures resemble niobium hydrides which were previously imaged using Bitter decoration in combination with SEM in a niobium single crystal [14].

The hydrides are known to grow on the niobium surface during the cool down process. They cause significant dissipation during the operation of SRF cavities [15, 16]. Therefore, all cavities undergo high temperature treatment to remove most of the dissolved gasses. The here presented sample was also sufficiently degassed however the mechanical polishing with use of a small amount of hydrogen peroxide most likely reintroduced hydrogen.

SUMMARY AND CONCLUSIONS

MO imaging was successfully applied to RRR300 niobium. It was shown that the obtained images give access to the distribution of trapped magnetic flux at the μm scale. Based on this technique, it was demonstrated that a high temperature treatment of the niobium leads to significantly reduced trapping though it was not completely eliminated. Approximately 30% of the applied magnetic field was trapped which is in accordance with previous macroscopic measurements [5]. The remaining trapped flux can be divided in two main contributions: An almost homogeneous background and localized centers with the size of the order of $10\ \mu\text{m}$.

The background level of trapped flux originates from different, homogeneously distributed pinning centers possibly including residual dissolved gases (e.g. oxygen) or lattice imperfections. Another likely explanation for the background signal is the damage layer on the very top of the sample. It arose from the final, mechanical polish and is expected to contribute to flux trapping. A subsequent study could use additional chemical polishing as the last processing step to remove the damage layer.

Due to the treatment history of the sample it provided the unique opportunity to directly compare the magnetic flux trapped by grain boundaries with the flux trapped by hydrides.

We found that hydrides lead to a local enhancement of trapped flux while the grain boundaries give no distinguishable contribution in the MO images.

The results indicate that impurities and dissolved gases could play a much stronger role as pinning centers than the grain size. Thus, the observed improvement of flux expulsion following a high temperature treatment may not primarily be caused by a change in morphology but by the reduction of dissolved gases.

Furthermore, the observations shed new light on the loss mechanism of hydrides during RF operation. Until now, hydrides have mainly been discussed in the context of the caused defects and their RF properties which lead to increased dissipation. Now, we understand, that the flux trapping aspect has to be included to gain a comprehensive picture.

Finally, it has to be acknowledged that SRF cavities are operated within ambient magnetic fields in the order of μT , not mT. While we have no indication that the conclusions drawn of the present study do not apply to lower magnetic field values as well, it has to be tested in subsequent studies.

ACKNOWLEDGMENTS

We would like to acknowledge Christiane Förster, HZB, for analyzing the crystal structure of the sample and for polishing of the Nb crystal. We also thank Axel Matheisen and colleagues from DESY who performed the chemical polishing of the samples, as well as Tobias Junginger and colleagues from TRIUMF where the sample was heat treated.

REFERENCES

[1] A. Gurevich and G. Ciovati, *Phys. Rev. B*, vol. 87, p. 054502 2013.

- [2] J.-M. Vogt, O. Kugeler, and J. Knobloch, *Phys. Rev. ST Accel. Beams*, vol. 16, p. 102002, 2013.
- [3] J.-M. Vogt, O. Kugeler, and J. Knobloch, *Phys. Rev. ST Accel. Beams*, vol. 18, p. 042001, 2015.
- [4] R. Eichhorn *et al.*, *Phys. Rev. Accel. Beams*, vol. 19, p. 12001, 2016.
- [5] S. Aull, O. Kugeler, and J. Knobloch, *Phys. Rev. ST Accel. Beams*, vol. 15, p. 062001, 2012.
- [6] A. Romanenko, A. Grassellino, A. Crawford, D. Sergatskov, and O. Melnychuk, *Applied Physics Letters*, vol. 105, p. 234103, 2014.
- [7] S. Posen, *et al.*, *Journal of Applied Physics*, vol. 119, p.213903, 2016.
- [8] T. Matsushita, “Flux Pinning in Superconductors”, Springer Series in Solid-State Sciences No. 178, Springer, 2014.
- [9] J. Köszegei, *et al.*, “Towards the perfect Meissner state: A magneto-optical study on magnetic flux expulsion and pinning in high-purity niobium”, submitted for publication.
- [10] A. Polyanskii, P. Lee, *et al.*, in *AIP Conference Proceedings*, vol. 1352, pp. 186-202.
- [11] M. Wang, *et al.*, *Proceedings of SRF2015*, pp. 120-124.
- [12] T. H. Johansen and D. Shantsev, eds., “Magneto-Optical Imaging”, vol. 1, Springer Netherlands, 2004.
- [13] R. Schäfer, “Investigation of domains and dynamics of domain walls by the magneto-optical Kerr-effect”, in *Handbook of Magnetism and Advanced Magnetic Materials*, John Wiley & Sons, Ltd, 2007.
- [14] L. Y. Vinnikov and A. O. Golubok, *physica status solidi (a)*, vol. 69, p.631, 1982.
- [15] B. Bonin and R. Roth, *Proceedings of the 5th Workshop on RF Superconductivity*, pp. 210.
- [16] J. Knobloch, *AIP Conference Proceedings 671*, pp.133.